2010-08

Investigation in SrTi'O IND.3'-CaTi'O IND.3'-PbTi'O IND.3' ternary thin films by dielectric proprieties and Raman spectroscopy

Journal of Sol-Gel Science and Technology,New York : Springer,v. 55, n. 2, p. 151-157, Aug. 2010
http://www.producao.usp.br/handle/BDPI/50074

J Sol-Gel Sci Technol (2010) 55:151–157
DOI 10.1007/s10971-010-2227-4

ORIGINAL PAPER

Investigation in $SrTiO_3$-$CaTiO_3$-$PbTiO_3$ ternary thin films by dielectric proprieties and Raman spectroscopy

D. S. L. Pontes · E. Longo · F. M Pontes · Marcelo A. Pereira-da-Silva · J. H. D. da Silva · A. J. Chiquito · P. S. Pizani

Received: 5 March 2010 / Accepted: 17 April 2010 / Published online: 1 May 2010

Abstract Dielectric and Raman scattering experiments were performed on polycrystalline $Pb_{1-x-y}Ca_xSr_yTiO_3$ thin films as a function of temperature. Temperature-dependent dielectric measurements revealed a decreasing ferroelectric-to-paraelectric phase transition temperature and peak dielectric permittivity showed a broad phase transition near room temperature with increasing levels of CaO_{12} and SrO_{12} clusters. Therefore, for higher levels of substitution, the possible random position of the CaO_{12} and SrO_{12} clusters leads to a diffuse state. At 100 kHz, the ferroelectric-to-paraelectric phase transition temperatures were 633, 495 and 206 K for PCST90 ($Pb_{0.90}Ca_{0.05}Sr_{0.05}TiO_3$), PCST70 ($Pb_{0.70}Ca_{0.15}Sr_{0.15}TiO_3$) and PCST30 ($Pb_{0.30}Ca_{0.35}Sr_{0.35}TiO_3$) thin films, respectively. The evolution of the Raman spectra was also studied as a function of temperature. The temperature dependence of the E(1TO) soft mode frequencies was used to characterize the phase transition. Raman peaks were observed above the ferroelectric-to-paraelectric phase transition temperature, although all optical modes should be inactive in Raman scattering. The origin of these modes was interpreted as a breakdown of the local cubic symmetry by the random distribution of CaO_{12} and SrO_{12} clusters.

Keywords Thin films · Phase transition · Ferroelectric · Raman spectroscopy

D. S. L. Pontes · E. Longo
Chemistry Institute, Universidade Estadual Paulista (UNESP), P.O. Box 355, Araraquara, SP 14801-970, Brazil

F. M Pontes (✉)
Department of Chemistry, Universidade Estadual Paulista (UNESP), P.O.Box 473, Bauru, SP 17033-360, Brazil
e-mail: fenelon@fc.unesp.br

M. A. Pereira-da-Silva
Instituto de Física de São Carlos, USP, São Carlos, SP 13560-250, Brazil

M. A. Pereira-da-Silva
Centro Universitário Central Paulista (UNICEP), São Carlos, SP 13563-470, Brazil

J. H. D. da Silva
Advanced Materials Group, Physics Department, São Paulo State University-UNESP, Bauru, SP 17033-360, Brazil

A. J. Chiquito · P. S. Pizani
Department of Physics, UFSCar, Via Washington Luiz, km 235, São Carlos, SP CEP-13565-905, Brazil

1 Introduction

Ferroelectric thin films continue to attract much attention in theoretical and experimental investigations due to their interesting practical applications in memory devices, infrared sensors, and piezoelectric sensors and actuators [1–3].

Despite the existence of various compound ferroelectric thin films, the main advantage of the $PbTiO_3$ perovskite structure is that it can readily display a variety of structural phase transitions. Such transitions can be achieved by replacing the A (Pb^{2+}) and/or (Ti^{4+}) B elements by other A′ and/or B′ elements in AO_{12} and/or BO_6 sites with different radii and charges, thereby forming other types of compounds, i.e., $PbZr_{1-x}Ti_xO_3$ (PZT), $Pb_{1-x}Ca_xTiO_3$ (PCT), $Pb_{1-x}Sr_xTiO_3$ (PST), $Pb_{1-x}Ba_xTiO_3$ (PBT), $PbNb_{0.04}Zr_{0.28}Ti_{0.68}O_3$ (PNZT), $Pb_{1-x}La_xZr_{1-y}Ti_yO_3$ (PLZT), and $Pb_{0.25}Ba_xSr_{0.75-x}TiO_3$ (PBST) [4–11]. It is also interesting to note that many ferroelectric materials, including $PbTiO_3$, exhibit relaxor behavior as a function of the type and concentration of dopant. This phenomenon is manifested by a strong

frequency dispersion of the dielectric constant at temperatures around the phase transition temperature [12, 13]. These materials show a relaxation-type phase transition. Lead magnesium niobate (PMN), lead zinc niobate (PZN), $Pb(Sc_{1/2}Nb_{1/2})O_3$ (PSN) and their solid solutions with lead titanate (PT) are the most widely studied relaxor materials [14–18]. In addition, with the increasing emphasis on ferroeletric thin films for various applications, especially memory storage devices, it is becoming increasingly important to understand the phenomenon of phase transitions in ferroelectric thin films. Vanderbilt and Zhong [19] applied the first-principles theory in a theoretical study of the ferroelectric phase transition of three cubic perovskite compounds, $SrTiO_3$, $CaTiO_3$ and $NaNbO_3$. Recently, Sun et al. [6] reported on the preparation and characterization of $Pb_{0.25}Ba_xSr_{0.75-x}TiO_3$ thin films with x = 0.05, 0.1, 0.15 and 0.2 on $Pt/Ti/SiO_2/Si$ substrates, pointing out that the structural, microstructural and electrical properties were strongly dependent on the Ba content. Currently, special attention focuses on the preparation of ternary compounds using materials with a perovskite structure. For example, Zhang et al. [20] reported on the preparation and characterization of $BaTiO_3$-$CaTiO_3$-$SrTiO_3$ (BSCT) ceramics, while Li et al. [21] analyzed the effect of $(Ca_{1-2x}Na_xLa_x)TiO_3$ A-site substituted perovskite compounds on the structure of the phase transition at room temperature. Abdelmoula et al. [22] showed that the simultaneous substitution of Ba^{2+} ions in the A-site by Sm^{3+} and Na^+ ions had a significant effect on the dielectric behavior. These authors reported that the material showed a classic ferroelectric phase transition at $0 \leq x \leq 0.10$ and $x \geq 0.50$, while a relaxor ferroelectric phase transition occurred at $0.20 \leq x < 0.40$.

So far no detailed study aimed at investigating the temperature dependence of the dielectric permittivity and Raman spectra of $Pb_{1-x-y}Ca_xSr_yTiO_3$ thin films has been reported.

2 Experimental procedure

Our procedure for synthesizing $Pb_{1-x-y}Ca_xSr_yTiO_3$ (abbreviated as PCST) thin films consisted of producing a polymeric resin using the soft chemistry method known as the polymeric precursor route. Details of the preparation method can be found in the literature [23].

The viscosity of the deposition solutions was adjusted to 12 mPa/s. After preparing the polymeric precursor, the solution was spin-coated onto 10 × 10 mm substrates [$Pt/Ti/SiO_2/Si$] using a commercial spinner operating at 7000 rev./min for 20 s (spin-coater KW-4B, Chemat Technology) and equipped with a syringe filter to avoid particulate contamination. A two-stage heat treatment was carried out as follows: initial heating at 400 °C for 4 h at a heating rate of 5 °C/min in an air atmosphere to pyrolyze the organic materials, followed by heating at 600 °C for 4 h at a heating rate of 5 °C/min for crystallization. These steps were repeated four times to obtain the desired thickness of about 180–240 nm.

Electrical measurements were taken of PCST90 ($Pb_{0.90}Ca_{0.05}Sr_{0.05}TiO_3$), PCST70 ($Pb_{0.70}Ca_{0.15}Sr_{0.15}TiO_3$) and PCST30 ($Pb_{0.30}Ca_{0.35}Sr_{0.35}TiO_3$) thin films with thicknesses of 180, 230 and 240 nm, respectively. The temperature-dependent dielectric constant of the thin films was studied in a metal-ferroelectric-metal configuration and the films were characterized using a $G^{w}_{\underline{}}$ Instek LCR 819 m at temperatures ranging from 50 to 663 K. For these measurements, circular Au electrodes with an area of approximately 4.9×10^{-2} mm^2 were deposited (using a shadow mask) by evaporation on the surfaces of the heat-treated films, serving as top electrodes. The measurements of the temperature-dependent dielectric constant of the PCST30 thin films were taken at temperatures varying from 50 to 300 K, using a closed-cycle helium cryostat.

The Raman measurements were taken with a T-64000 Jobin–Yvon triple-monochromator coupled to a charge-coupled detector (CCD). An optical microscope with a 50X objective was used to focus the 514.5 nm line of a Coherent Innova 70 argon laser onto the sample. The laser output power was kept at about 20 mW. The thin films were mounted in a TMS 93 furnace (Linkam Scientific Instruments Ltd) with controlled temperature in the range of 298–773 K. In addition, low temperature Raman spectra were obtained using a closed-cycle helium refrigerator for the measurements in the 10–300 K temperature range.

3 Results and discussion

The phase transition temperature of the various PCST thin films is shown in Fig. 1. Several interesting features are apparent from the dielectric constant (ε) versus temperature curves of the PCST90, PCST70 and PCST30 thin films with different Ca^{+2} and Sr^{2+} concentrations. As can be seen (see Fig. 1), the phase transition of the PCST90 thin film from ferroelectric to paraelectric was rather sharp and occurred at around 633 K. However, there is a tendency for the maximum peak of the dielectric constant to broaden as the concentration of in Ca^{2+} and Sr^{2+} increase in the A-site, indicating that the phase transition may be of a diffuse type close to the transition temperature. Recently, Ke et al. [23] used a Lorentz-type relation to describe the dielectric permittivity of the normal ferroelectric with or without diffuse phase transition in perovskite ceramics samples of the type $Ba(Zr_xTi_{1-x})O_3$, PMN and $BaTiO_3$.

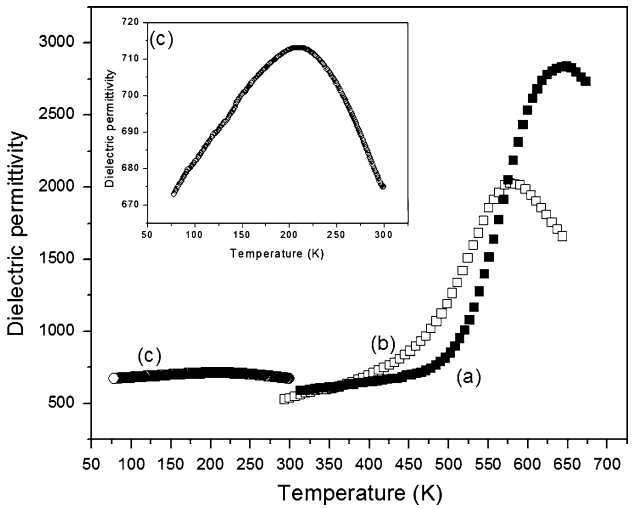

Fig. 1 Temperature dependence of dielectric permittivity for PCST thin films measured at 100 kHz. (*a*) PCST90, (*b*) PCST70 and (*c*) PCST30

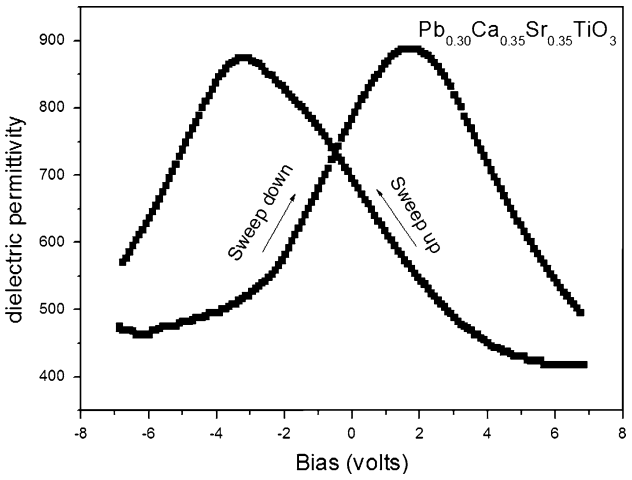

Fig. 2 Bias dependence of dielectric permittivity measurements at low temperature 50 K for PCST30 thin films

It is known that a sharp or diffuse phase transition in material with an ABO_3 perovskite structure is more dependent on the electronic charge density in the octahedral and dodecahedral sites, BO_6 and AO_{12}, respectively. In all the PCST thin films, the A-site showed a 12-fold oxygen coordination containing three types of PbO_{12}, CaO_{12} and SrO_{12} clusters. The random distribution of these clusters in the A-site leads to heterogeneity of the nanoscale composition in thin films, thus inducing a broadening of the phase transition peak. As Fig. 1 shows, the PCST90 and PCST70 thin films displayed a Curie temperature above room temperature, i.e., 633 and 495 K, respectively, indicating their ferroelectric nature at room temperature. On the other hand, the PCST30 thin films exhibited a stronger signature of typical diffuse phase transition behavior, with its maximum at a temperature of about 206 K. This temperature is related to the ferroelectric-to-paraelectric phase transition temperature.

Figure 2 shows the characteristic dielectric permittivity-bias curves of the PCST30 thin films measured at around 50 K. The curve shows typical hysteresis behavior, indicating that the dielectric thin film has a ferroelectric property at lower temperatures. Furthermore, the hysteresis behavior increased as the temperature decreased, indicating that the dipolar clusters continued to grow during cooling to room temperature, and suggesting that the disorder of the CaO_{12}, SrO_{12} and PbO_{12} localized in the AO_{12}-site favors the randomization of the orientation of the Ti–O dipolar cluster. These randomly distributed domains then cause a large range of phase transition temperatures.

On the other hand, PCST30 thin films have a Curie temperature below room temperature, which is indicative of the paraelectric nature of PCST30 thin films at room temperature. Shao et al. [24] also reported a diffuse phase transition for complex $Pb_{0.40}Sr_{0.60}Zr_{0.52}Ti_{0.48}O_3$ (PSZT) thin films on Pt/Si substrates, with a maximum at a temperature of 204 K. By comparison with previously published results of the temperature-dependence of the dielectric constant of $Pb_{1-x}Ca_xTiO_3$ and $Pb_{1-x}Sr_xTiO_3$ films, we also identified a diffuse-type phase transition as a function of Ca and Sr content [12, 25–30]. Table 1 summarizes the values of the phase transition temperature obtained for the PCST, PCT and PST thin films.

It is a well known fact that perovskite-type relaxor ferroelectric thin films are characterized by the diffuse nature of their ferroelectric-to-paraelectric phase transition and by their frequency-dependent transition temperature.

Table 1 Phase transition temperature obtained by electrical measurements of PCST thin films herein obtained and compared with another PCT and PST thin films according to the literature

Sample	Phase transition temperature (K)	Reference
$Pb_{0.90}Ca_{0.05}Sr_{0.05}TiO_3$	650	This work
$Pb_{0.70}Ca_{0.15}Sr_{0.15}TiO_3$	570	This Work
$Pb_{0.30}Ca_{0.35}Sr_{0.35}TiO_3$	206	This Work
$Pb_{0.90}Ca_{0.10}TiO_3$	688	27
$Pb_{0.80}Ca_{0.20}TiO_3$	623	27
$Pb_{0.70}Ca_{0.30}TiO_3$	533	27
$Pb_{0.60}Ca_{0.40}TiO_3$	463	27
$Pb_{0.76}Ca_{0.24}TiO_3$	573	28
$Pb_{0.50}Sr_{0.50}TiO_3$	413	29
$Pb_{0.30}Sr_{0.70}TiO_3$	288	30
$Pb_{0.70}Sr_{0.30}TiO_3$	573	31
$Pb_{0.60}Sr_{0.40}TiO_3$	463	32
$Pb_{0.40}Sr_{0.60}TiO_3$	343	32

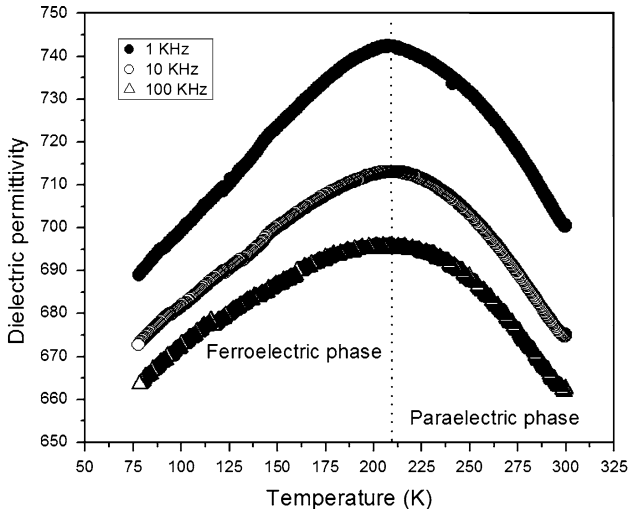

Fig. 3 Temperature and frequency dependence of dielectric permittivity for PCST30 thin films

Therefore, Fig. 3 shows the temperature dependence of the dielectric constant of PCST30 thin films at different frequencies. Figure 3 shows the value of the dielectric constant increasing gradually to a maximum value as the temperature rises to the phase transition temperature and thereafter decreasing, indicating a phase transition. For the PCST30 thin films, the dielectric constant maximum and the corresponding temperature maximum were independent of the measured frequency. This particular property is typical of classical ferroelectric thin films. All the compositions showed similar characteristics, indicating that these compounds are of the classical ferroelectric type. However, for typical relaxor, there is a strong frequency dependence of the temperature corresponding to maximum permittivity in agreement with the studies accomplished by Ke et al. [23].

Another important point about the PCST thin films is that their phase transition temperature shifted downward in response to simultaneous increases in randomly connected CaO_{12} and SrO_{12} clusters in the AO_{12} sites, which may be attributed to factors such as cluster size, coordination and configuration. As many researchers well know, the dipoles that allow for the ferroelectric effect in $PbTiO_3$ perovskite occur through these slightly distorted TiO_6 octahedral clusters, which give rise to polar macro, micro and nano-regions. In addition to the $PbTiO_3$ perovskite structure, the stronger distortion of the octahedron lead to the high polarizability of PbO_{12} clusters and the possibility that they become strongly deformed in an electric field; hence, PbO_{12} clusters are strongly polar. The origin of this polarity is based on the partial alignment of local PbO_{12} clusters. These effects give rise to a highly distorted unit cell. Therefore, the presence of SrO_{12} and CaO_{12} clusters of different sizes and electronic configurations than the PbO_{12} cluster in the A-site perovskite structure caused an abrupt drop in the phase transition temperature. This effect on the phase transition temperature may be correlated with the contribution of new SrO_{12} and CaO_{12} clusters in the crystalline lattice, which induced: (1) a relative reduction of the unit cell volume; (2) consequently, a weaker distortion of the octahedron; and (3) formation of nonpolar clusters in which the long-range Ti–O dipoles disappear at room temperature.

To study the ferroelectric-to-paraelectric phase transition by Raman spectroscopy, Raman spectra of $Pb_{1-x-y}Ca_xSr_yTiO_3$ thin films were obtained at different temperatures, and the results are shown in Figs. 4, 5 and 6. An examination of Raman scattering profiles of PCST90

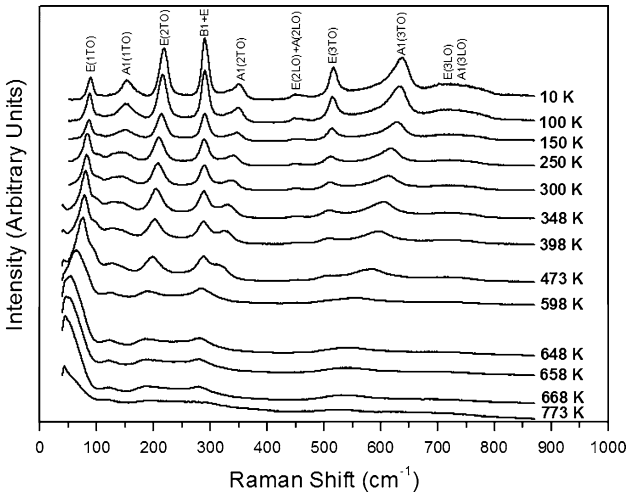

Fig. 4 Raman spectra of $Pb_{0.90}Ca_{0.05}Sr_{0.05}TiO_3$ (PCST90) thin films at various temperatures

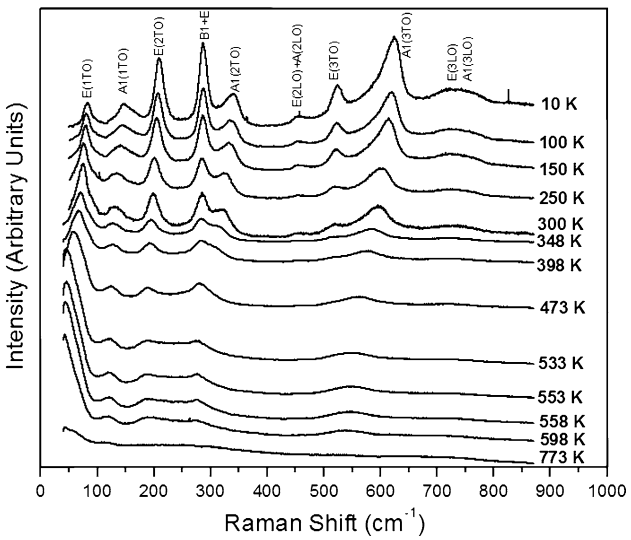

Fig. 5 Raman spectra of $Pb_{0.70}Ca_{0.15}Sr_{0.15}TiO_3$ (PCST70) thin films at various temperatures

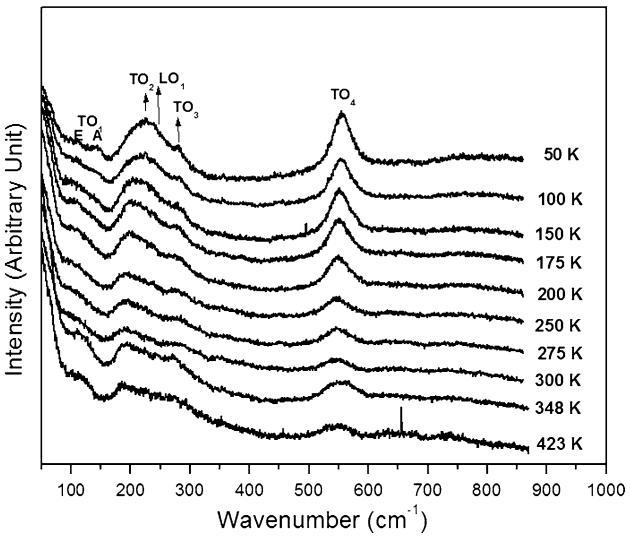

Fig. 6 Raman spectra of $Pb_{0.30}Ca_{0.35}Sr_{0.35}TiO_3$ (PCST30) thin films at various temperatures

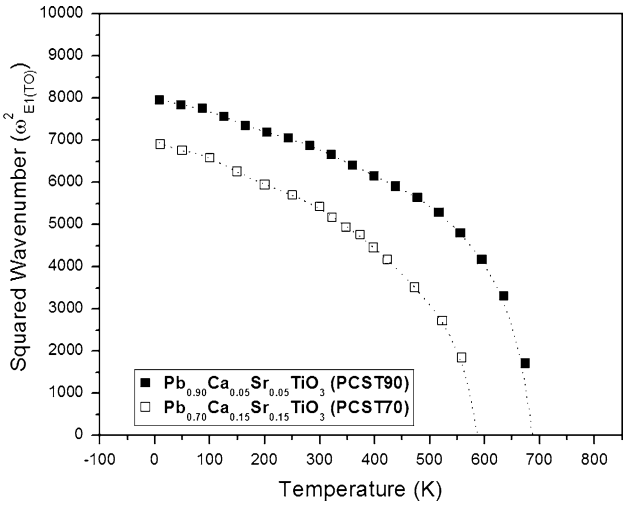

Fig. 7 Temperature dependence of the squared wave number of the soft E(1TO) mode in the PCST90 (*filled square*) and PCST70 (*open square*) thin films

and PCST70 thin films at 10 and 300 K reveals a qualitative similarity to the profiles observed in the $PbTiO_3$ thin films, showing all Raman active transversal and longitudinal optical modes, as expected for a tetragonal structure (*P4 mm* space group). Unlike the PCST90 and PCST70, the PCST30 exhibits only broad Raman peaks, indicating a high degree of local disorder from low to high temperatures. Furthermore, a important signature of the tetragonal ferroelectric-to-cubic paraelectric phase transition is the softening of the lowest-frequency mode (the *E(1TO)* soft mode), whose frequency tends to zero as it approaches the Curie temperature. For PCST90 and PCST70, these modes, located at 89 and 83 cm^{-1} at 10 K, respectively, clearly show a red shift indicating increasing temperature, as illustrated in Figs. 4 and 5. The temperature dependence of the square of the soft mode frequency is shown in Fig. 7. By extrapolating these curves, the transition temperature was estimated to be about 650 and 520 K for PCST90 and PCST70, respectively. In addition, Torgashev et al. [31] reported that single-crystal samples of the $Pb_{0.50}Ca_{0.50}TiO_3$ solid solution undergoes two phase transitions at 392 K (T_1) and 452 K (T_2).

The effect of temperature on the all Raman modes of PCST90 and PCST70 is shown in Fig. 8. Two distinct behaviors can be identified in this figure: modes slightly sensitive to temperature changes—E(2TO), B1 + E, E(2LO) + A(2LO), E(3TO)—and modes highly sensitive to temperature changes—A_1(3TO) and A_1(2TO)—showing a significant red shift to increasing temperature, a behavior normally attributed to the coupling of these modes with the E(1TO) soft mode. In the particular case of A_1(3TO) mode, both Ti and O ions move against Pb ions along the z direction in BO_6-type clusters [32]. Hence, the frequency of the mode may be affected by the contents of new CaO_{12} and SrO_{12}-type clusters.

For temperatures above Tc, in which the optical modes should be inactive in Raman scattering, broad Raman bands are still visible for the three compositions. The presence of such Raman peaks in the globally averaged cubic or pseudocubic phase can be attributed to local structural disorder. This effect has been observed frequently in materials with a high degree of chemical disorder, particularly in short-range localized polar entities arising from randomly distributed CaO_{12} and SrO_{12} clusters. This reflects the fact that more than one kind of dodecahedral cluster competes for the A-site in $PbTiO_3$ (for example, PbO_{12}, CaO_{12} and SrO_{12}). These randomly connected CaO_{12} and SrO_{12} clusters destroy the perfect local cubic symmetry, causing the breakdown of Raman selection rules. Forbidden polar modes were also observed in the PCST30 thin film paraelectric phase far above the phase transition temperature, although they were very weak at room temperature and the second-order contribution dominated. Therefore, in the case of the PCST30 thin films, the presence of Raman lines should be attributed to the noncubic local structure at and below room temperature. This distorted or noncubic local structure was not detected by XRD and FT-IR analysis, but it was visible in the Raman spectra through the presence of symmetry-forbidden Raman lines. Furthermore, in the case of PCST30, X-ray diffraction and FT-IR analyses at room temperature suggested that the structural phase was most likely the $SrTiO_3$ perovskite cubic structure. Also, in the case of PCST30 thin films, an analysis of the evolution of the Raman spectra depicted in Figs. 6 and 9 indicates that all the Raman lines were present and remained almost temperature-independent in

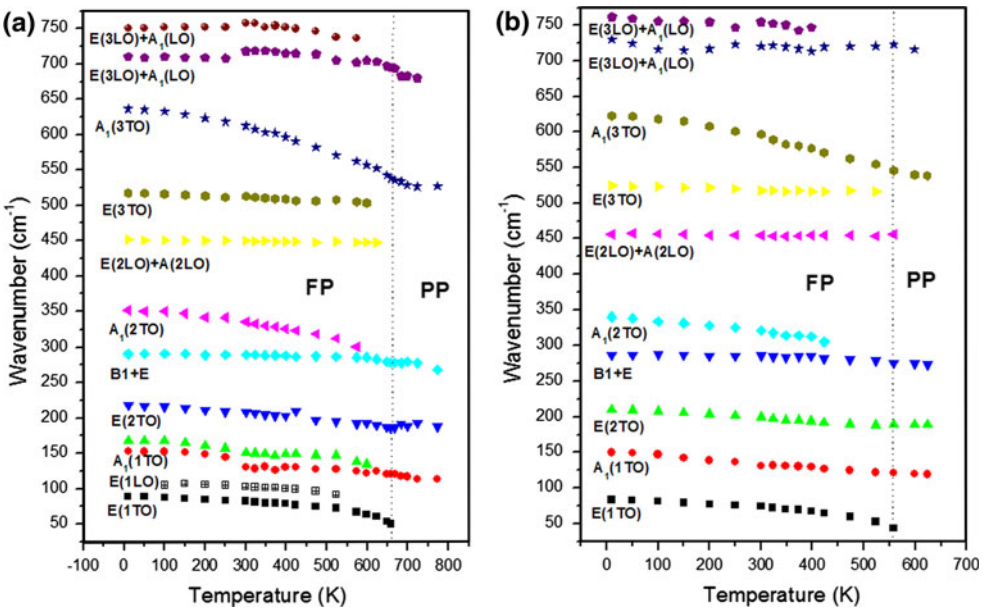

Fig. 8 Variation in Raman shifts as a function of temperature for **a** PCST90 and **b** PCST70 thin films. *FP* ferroelectric phase (*tetragonal*), *PP* paraelectric phase (*pseudocubic*)

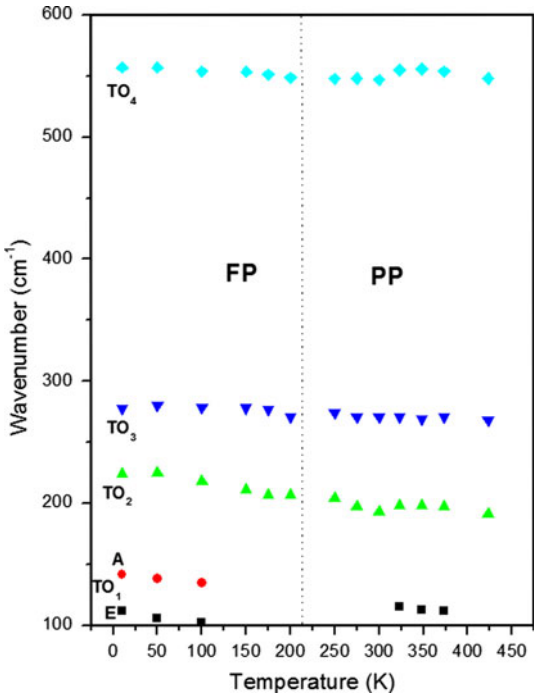

Fig. 9 Variation in Raman shifts as a function of temperature for PCST30 thin films. *FP* ferroelectric phase, *PP* paraelectric phase

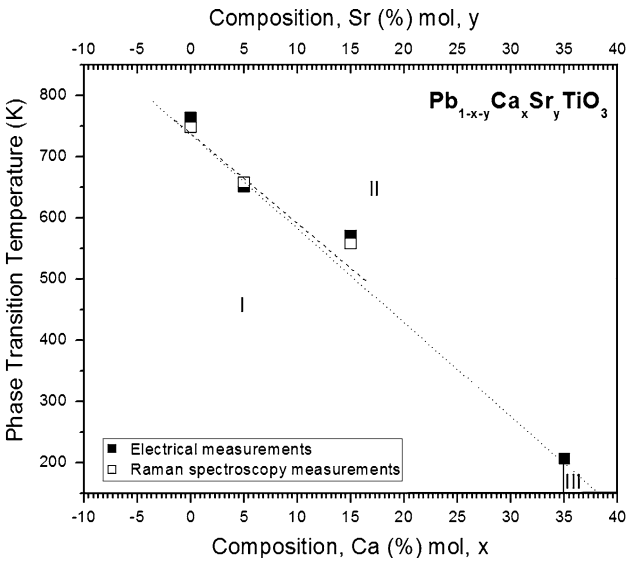

Fig. 10 Phase diagram obtained by phase transition temperature for $Pb_{1-x-y}Ca_xSr_yTiO_3$ thin films as observed using temperature dependent Raman scattering and electrical methods. *Region I* tetragonal-ferroelectric phase; *Region II* pseudocubic-paraelectric phase and *Region III* tetragonal-ferroelectric phase

the 10–300 K range. Further investigations are needed to understand the effects in cosubstituted PCST30 multi-clusters in order to determine the phase transition temperature through Raman studies.

Figure 10 shows a phase diagram for the PCST90, PCST70 and PCST30 thin films based on the results of the dielectric and Raman measurements as a function of temperature.

4 Conclusions

In summary, we demonstrated the strong influence of CaO_{12} and SrO_{12} clusters on the temperature-dependent structural and dielectric properties of $Pb_{1-x-y}Ca_xSr_yTiO_3$ (PCST) thin films. The dielectric study revealed that the dielectric permittivity peak in PCST90 and PCST70 thin films is fairly sharp, unlike that of PCST30 thin films, where the phase transition becomes diffuse without

frequency dependence: this is a typical ferroelectric-to-paraelectric phase transition. The diffuseness increased with increasing contents of CaO_{12} and SrO_{12} clusters in the dodecahedral-site. This phenomenon is likely related with the existence of short-range localized polar domains, since the possible random positions of CaO_{12} and SrO_{12} clusters in the A-site favor randomization of the octahedral dipoles, leading to nanoscale dipolar heterogeneity. The phase transition temperature decreases with increasing CaO_{12} and SrO_{12} cluster contents due to the decreasing polarity of these clusters.

Raman spectroscopy was employed to study the effect of the substitution of CaO_{12} and SrO_{12} clusters on the structural properties as a function of temperature. Structural analyses of the PCST thin films by Raman spectroscopy revealed a decrease in the tetragonal distortion of the unit cell with an increase in CaO_{12} and SrO_{12} cluster content. Accordingly, a decrease in the ferroelectric phase transition temperature was detected by temperature-dependent Raman spectroscopy. The phase transition temperature of the PCST90 and PCST70 thin films was estimated using the softening of the $E(1TO)$ mode of the tetragonal phase. Unlike the dielectric permittivity measurements, the PCST30 thin films showed a diffuse Raman scattering response, making it difficult to estimate the phase transition temperature. In the PCST30 thin films, the substitution of CaO_{12} and SrO_{12} clusters resulted in a Raman spectrum with broad bands, which are characteristic of a highly structured locally disordered material.

Acknowledgments This work was financially supported by the Brazilian agencies FAPESP/CEPID, CNPq and CAPES. FAPESP process n°. 06/53926-4, 06/51640-6 and 08/53515-7.

References

1. Guo YP, Akai D, Sawada K, Ishida M, Gu M (2009) J Sol-Gel Sci Technol 49:66
2. Karan NK, Thomas R, Pavunny SP, Saavedra-Arias JJ, Murari NM, Katiyar RS (2009) J Alloys Comp 482:253
3. Higuchi T, Yamasaki T, Suzuki Y, Gotoh K, Hattori T, Tsukamoto T (2008) J Appl Phys 103:84108
4. Soon HP, Wang J (2006) J Electroceram 16:277
5. Shannigrahi S, Yao K (2005) Appl Phys Lett 86:92901
6. Sun X, Huang H, Wang S, Li M, Zhao X-z (2008) Thin Solid Films 516:1308
7. Nagaraj B, Aggarwal S, Ramesh R (2001) J Appl Phys 90:375
8. Wang SX, Hao JH, Wu ZP, Wang DY, Zhuo Y, Zhao XZ (2007) Appl Phys Lett 91:252908
9. Negi NS, Sharma DR, Rastogi AC (2008) J Phys Chem Sol 69:41
10. Yang WD, Haile SM (2006) J Eur Ceram Soc 26:3203
11. Chen L, Shen M, Fang L, Xu Y (2008) Thin Solid Films 516:1285
12. Yang J, Chu J, Shen M (2007) Appl Phys Lett 90:242908
13. Sayouri S, Kellati M, Taibi MM, Moudden NEl, Tlemcani M, Ghazouali AEl, Kaal A (2004) Phys Stat Sol A Appl Res 201:3001
14. Asanuma S, Uesu Y, Malibert C, Kiat JM (2008) J Appl Phys 103:94106
15. Li YW, Hu G, Yue FY, Yang GY, Shi WZ, Meng XJ, Sun JL, Chu JH (2007) Appl Phys Lett 91:232912
16. Ching-Prado E, Cordero J, Katiyar RS, Bhalla AS (1996) J Vac Sci Technol A 14:762
17. Paik DS, Park SE, Wada S, Liu SF, Shrout TR (1999) J Appl Phys 85:1080
18. Kholkin AL, Akdogan EK, Safari A, Chauvy PF, Setter N (2001) J Appl Phys 89:8066
19. Vanderbilt D, Zhong W (1998) Ferroelectrics 206:81
20. Zhang L, Wang X, Yang W, Liu H, Yao X (2008) J Appl Phys 104:14104
21. Li Y, Qin S, Seifert F (2007) J Sol St Chem 180:824
22. Abdelmoula N, Chaabane H, Khemakhem H, Von der Mühll R, Simon A (2006) Solid State Sciences 8:880
23. Ke S, Fan H, Huang H, Chan HLW (2008) Appl Phys Lett 93:112906
24. Shao QY, Li AD, Dong Y, Fang F, Jiang JQ, Liu ZG (2007) J Phys D Appl Phys 40:3793
25. Pontes DSL, Longo E, Pontes FM, Galhiane MS, Rissato SR, Santos LS, Leite ER (2008) J Phys Chem Sol 69:1951
26. Pontes FM, Pontes DSL, Leite ER, Longo E, Pizani PS, Chiquito AJ, Machado MAC, Varela JA (2004) Appl Phys A Mater Sci Proc 78:349
27. Pontes FM, Pontes DSL, Leite ER, Longo E, Pizani PS, Chiquito AJ, Varela JA (2003) J Appl Phys 94:7256
28. Zhou D, Wu W, Jin D, Cheng J, Meng Z (2008) IEEE Trans Ultras Freq Cont 55:1034
29. Pontes FM, Leal SH, Leite ER, Longo E, Pizani PS, Chiquito AJ, Varela JA (2004) J Appl Phys 96:1192
30. Zhai J, Yao X, Xu Z, Chen H (2006) J Appl Phys 100:34108
31. Torgashev VI, Yuzyuk IY, Shirokov VB, Lemanov VV (2006) Phys Solid State 48:919
32. Freire JD, Katiyar RS (1988) Phys Rev B 37:2074